Regular article

Solvation effects on cation–π interactions: a test study involving the quaternary ammonium ion

Carlo Adamo[1], Gaston Berthier[2], Roger Savinelli[3]

[1] Laboratoire d'Electrochimie et Chimie Analytique, UMR CNRS-ENSCP no. 7575, Ecole Nationale Supérieure de Chimie de Paris, 11 rue P. et M. Curie, 75231, Paris Cedex 05, France
[2] LETMEX, Museum National d'Historie Naturelle, 61, rue Buffon, 75005, Paris, France
[3] Laboratoire de Biochimie Théorique, Institut de Biologie Physico-Chimique, 13 rue P. et M. Curie, 75231 Paris, France

Abstract. Water solvation effects on theoretical binding energies of the tetramethylammonium cation with benzene, phenol and indole have been analyzed as a prototype of biological cation–π interactions. Solvent effects were introduced in the quantum chemical computations either by considering molecules belonging to the first solvation of the tetramethylammonium or by a polarizable continuum model. Our results show that the calculated binding energies are reduced by about three quarters with respect to the corresponding gas-phase results, but the sequence benzene < phenol < indole is preserved, in accordance with the concept of cation–π interactions. Similar results are obtained for the interaction of tetramethylammonium with the benzene–indole pair.

Introduction

The possibility for a biological role of the aromatic rings of phenylalanine, tyrosine and tryptophan interacting with onium ions by "cation–π" interaction was suggested early on the basis of various observations [1, 2]. Among those was the determination of the crystal structure of the phosphocholine-binding immunoglobulin FabMcPC60 [3] and the detection of numerous tyrosine and tryptophan residues in the region of binding of acetylcholine (ACh) on the surface of the nicotinic ACh receptor [4]. This proposal was strengthened by

the discovery, in the X-ray structure of the enzyme acetylcholinesterase, of 14 aromatic residues along the walls of a narrow gorge leading to the binding site of the substrate (ACh) [5]; thereby the suggestion that this could help the molecule to slide down to the active site along a series of low-affinity sites involving aromatic–quaternary ammonium interactions[6].

A computation of the interaction energy of a flexible ACh molecule with a model of the gorge (built on the X-ray coordinates) indeed revealed the existence of a succession of local sites of increasing energy, culminating at the binding site [7]. Within the limits of the model, the analysis of the structures of these sites provides insight into the respective roles and of other key residues (see Ref. [8] for a detailed discussion).

Much interest has developed in the last few years in achieving better understanding of the cation–π interaction, and this has resulted in a number of quantum mechanical calculations on simplified systems modeling biological processes [9]. From a series of correlated post-Hartree–Fock computations with rather flexible basis sets [10, 11, 12, 13] using mainly tetramethylammonium (TMA) as a simple model for ACh and small aromatic molecules (benzene, phenol and indole) as models for the aromatic amino acid receptors phenylalanine, tyrosine and tryptophan, we drew the following conclusions:

1. TMA is a good model for the ACh–benzene interaction.
2. The sequence of the TMA binding energy with the aromatic receptors is benzene < phenol < indole, while a single atomic ion, like Na^+, gives much larger values.
3. According to second-order Møller–Plesset (MP2) computations, TMA in its stablest arrangement with respect to benzene has a binding energy in fair agreement with the value measured in the gas phase (9.1 versus 9.4 kcal mol^{-1} [1]).

Correspondence to: G. Berthier
e-mail: gberthier@mnhn.fr

4. The partition of the binding energy between its Hartree–Fock components, essentially due to the purely Coulombic interaction of the TMA and benzene charge distribution, and the MP2 one, mainly associated with dispersion forces, is about 2/3–1/3 [11]. This point is of particular importance in view of the past discussions on the nature of such interactions (i.e. electrostatic versus dispersion) [14].

The preceding works were carried out for systems in the gas phase, the question of solvation being generally neglected in these quantum-mechanical investigations. However, the role of water, which may be of great importance in the ACh-aromatic interaction phenomena owing to its universal presence in biological systems, was considered in calculations concerning the location of H_2O molecules fixed on ACh hydrate and the related conformation problem [15]. Besides, computer simulation studies using molecular mechanics potentials have been performed in order to clarify the question of the hydration of hydrophobic substrates such as benzene [16, 17, 18, 19].

Here we have tried to elucidate this problem by means of new quantum-mechanical calculations including solvation effects. Two different approaches to this problem have been considered. In the first one, the solute with the surrounding solvent molecules (strongly bonded to it) was included in the quantum chemical computations, while in the second the solvent was modeled by the polarizable dielectric continuum of Scrocco and Tomasi [20, 21] (for a comprehensive review see Refs. [22, 23]). In such an approach the solvent is described by a polarizable continuum medium (PCM) representing, in an average way, all the possible accessible conformations to the solvent molecule, while the radial distribution is a "step" function [24]. This model provides accurate results for molecular properties and thermodynamics quantities in a nonpolar environment, while it catches the major part of solute–solvent interactions in polar, hydrogen-bonded liquids [25, 26, 27, 28, 29].

Computational details

All the complexes investigated in this study were treated in the frame of the so-called supermolecule approach, by calculating the interaction energy of the two entities A and B inside the total energy AB. In particular, electronic energies $E^0(AB)$ and $E^0(A) + E^0(B)$, basis set superposition error (BSSE) corrections [30], and zero-point vibrational energies (ZPVE) were evaluated, as well as PCM corrections. As in our previous work, correlation was introduced at the self consistent-field (SCF) MP2 level of theory [31], using completely optimized structures for the individual molecules A and B and a partial determination of geometry in the case of the whole complex AB, i.e. the relative disposition of its two components A and B. In order to verify this last point, a complete optimization was carried out only for phenol, owing the flexibility of the OH tail.

All the computations, including the MP2 ones, were performed with a slightly modified 6-31G(d,p) basis set. In this basis, denoted 6-31G^{aa} in Refs. [10, 11, 12, 13], the valence orbitals of the nitrogen atom in TMA were contracted by a scale factor of 1.09, obtained by minimizing the total energy of N^+. Polarization functions were also added, namely H(p), exp = 1.22; C(d), exp = 0.83; N(d), exp = 0.91; and O(d), exp = 0.99.

Concerning ZPVE corrections, the evaluation of relevant values made, as usual, at the SCF 6-31G level from harmonic frequencies scaled by a factor of 0.9 [32] deserves some attention in the present case. First of all, it is necessary to optimize all the geometrical parameters of the supermolecule AB, in order to avoid the occurrence of imaginary wave numbers polluting the remaining vibrational spectrum. As pointed out in an early paper on the water dimer [33], the total number of internal vibrational motions of an AB system is $3(N_A + N_B)-6$ for a complex built with N_A atoms from molecule A and N_B atoms from molecule B, instead of $(3N_A-6) + (3N_B-6)$. This includes the transformation of six translation–rotation motions of A and B, assumed to have zero energies in the vibrational treatment of the isolated molecules, into six vibrational motions of frequencies less than 100 cm^{-1}. To have an estimation of the upper and lower limits of the effects due to this change on ZPVE values, we computed them into two ways: first, in the standard manner with the $3N$-6 vibrational modes for the AB complex; second, by removing the 12 lower frequencies from the $3N$ set generated by the treatment of AB in Cartesian coordinates. For the systems considered in this work, the six lowest frequencies excluded from the second treatment give an almost constant contribution to the ZPVE correction originally computed, very similar to those quoted for the water dimer and equal to about half the total ZVPE differences. The magnitude of the total correction itself is not sufficient to alter the relative stability order of the various complexes. At the same time, the vibrational contribution of TMA was computed for its stablest conformation, with the hydrogen atoms in an eclipsed position with respect to the adjacent hydrogens, but in a staggered position with respect to the CN bonds (Fig. 1). All the other conformations accessible through a rotation along the CN bonds were not considered in the calculations of the interaction energy, since they correspond to first-order saddle points, quite high in energy ($+3.9$ kcal mol^{-1}).

Nonspecific solvent effects were evaluated using the original dielectric polarizable continuum model [20, 21] with cavities adapted to the shape of the molecule. These latter were determined
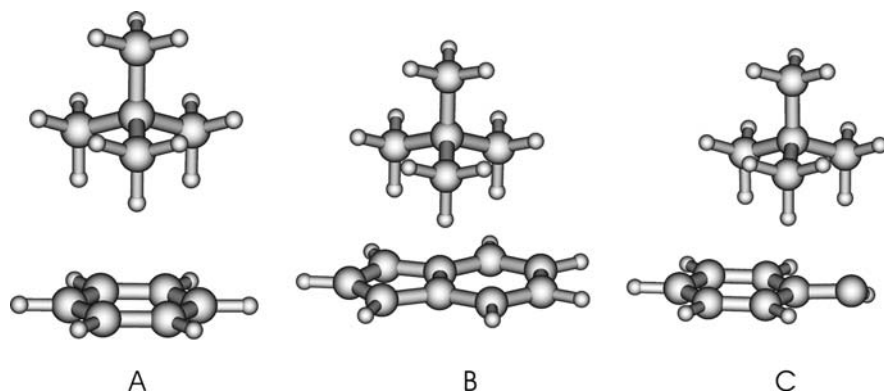

Fig. 1. Structure of the different complexes: **a** tetramethylammonium (*TMA*)–benzene; b TMA–indole; c TMA–phenol

by the united atom topological model [34] to determine the molecular cavity, instead of spheres in the Onsager theory or ellipsoids in the improved method of Rivail and Rinaldi [35]. The effect of outlying charge (the so-called "escaped charge" effect) was taken into account by means of an additional effective charge, distributed according to the solute electronic density [36].

All the computations were done by means of the Gaussian computer code [37]. They were carried out not only to calculate the binding energy of TMA, using benzene, phenol and indole as unique receptors, but also in the case of two receptors, benzene and indole, conveniently arranged in space, as in the natural product.

Results and comments

The structures of the complexes considered are depicted in Fig. 1. They correspond to the best gas-phase arrangement of TMA with the aromatic substrate as reported in Refs. [10, 12]: TMA is linked perpendicularly to the receptor through three hydrogens belonging to three different methyl groups in the case of benzene and indole, or in an oblique way in the case of phenol because of its interaction with the OH substituent. A similar arrangement has been obtained recently by density functional calculations on the TMA–benzene adduct [38].

As already mentioned, all the molecules (TMA, indole, benzene and phenol) were optimized separately, while only the distance between the nitrogen atom of TMA and the molecular plane of the aromatic molecules was relaxed in the supermolecular calculations.

Table 1. Tetramethylammonium (*TMA*)-aromatic ring distance (Å) for the complexes considered, computed at the second-order Møller–Plesset level, using the modified 6-31G(d) basis set (see text for details). The values corresponding to the complete optimization of the complex are reported in *parentheses*

	Adduct	Adduct + PCM	Adduct + $3H_2O$	Adduct + PCM + $3H_2O$
TMA–benzene	4.21	4.23	4.28	4.28
	(4.21)	(4.24)	(4.28)	(4.26)
TMA–phenol	4.43	4.49	4.50	4.52
TMA–indole	4.15	4.25	4.27	4.27

According to the data reported in Table 1, such a distance decreases in the order phenol > benzene > indole, the TMA–phenol distance being the largest (4.43 Å). As already stated, a full optimization of the geometrical parameters allowing us to check the effects of the TMA–aromatic interactions on the geometries of the different moieties was carried out for the TMA–benzene complexes. Only small variations (less than 0.002 Å) were found for all the intramolecular parameters, in agreement with recent computations also showing that the intramolecular bond lengths in the TMA–benzene complex do not change with respect to those characteristic of the isolated fragments [38]. At the same time, the N–ring distance practically does not change (less than 0.001 Å). All these results, as well as our previous calculations [10, 12], strongly suggest that the weak cation–Π interaction has practically no effect on the geometries of the two moieties.

The Mulliken charges of the TMA residues in the different complexes, computed at the equilibrium TMA–ring position, are reported in Fig. 2. As expected these charges are close to the formal +1 charges assumed for the ammonium salt, all ranging between +0.94 and +0.95|e⁻|. The negligible charge transfer found (less than 0.06|e⁻|) well underlines the role played by dispersion forces in this kind of interaction [10], especially when related to the magnitude of the interaction energies.

We give the interaction energies for all the species considered as well as all the different corrections (i.e. BSSE and ZPVE) in Table 2. An examination of these results indicates that these energies follow the order benzene < phenol < indole.

Our present results for the TMA–benzene complex, using a somewhat reduced basis set with respect to our precedent investigations, are close to those already reported using a larger basis set [13] and, when ZPVE and thermal correction (not reported in the table) are added, are close to the experimental values (8.0 versus 9.4 kcal mol⁻¹). This last result shows the kind of precision we also expected for the other complexes (indole
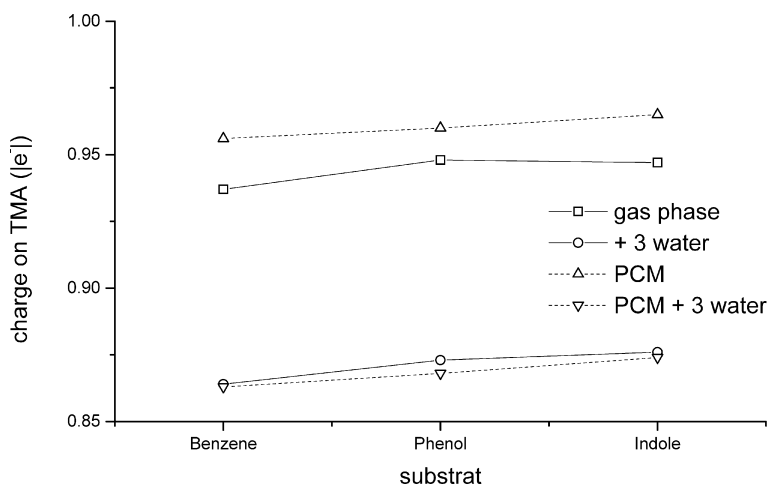

Fig. 2. Mulliken charges on the TMA fragment in the different adducts. The charges were evaluated either for the gas phase or for the different model solutions

Table 2. Different contributions to the interaction energies between TMA and the aromatic molecules considered (kcal mol^{-1}). The solvent contribution, ΔE_{solv}, was computed using the dielectric polarizable continuum model (*DPCM*) approach. Low and high vibrational contributions (ΔZPVE) to the binding energy (see text for details)

	Benzene	Phenol	Indole	Benzene–indole	
				With respect to benzene	With respect to indole
ΔE_{gas}	10.9	13.1	16.4	10.1	15.6
BSSE	−2.8	−3.8	−4.2	−3.2	−4.6
ΔE_{solv}	−7.0	−7.3	−9.6	−6.5	−9.0
Total	1.1	2.0	2.6	0.4	2.0
ΔZPVE (low/high)	−0.21/−0.54	−0.18/−0.54	−0.26/−0.57		

and phenol), for which no experimental data are available. We also note that the trend in the interaction energies is not clearly related to the differences in the intermolecular distance already discussed. Furthermore, the interaction energies practically do not change upon the complete optimization of the whole complex; for instance, the variation for the benzene–TMA interaction energy is less than 0.3 kcal mol^{-1}.

As a first step in the study of the solvation effect on our systems, we have represented the solvent as a dielectric continuum, thus modeling only the nonspecific solute–solvent interactions. The effects of the solvent reaction field on the intermolecular TMA–ring distance are reported in Table 1 (second column). As can be seen from these data, a small lengthening is observed for all systems, slightly more evident for the indole system (+0.1 Å) than for the other complexes. This behavior can be related to the stabilization, induced by the solvent, of the form with greater charge separation between the two fragments. In our case, this corresponds to the localization of a greater positive charge on TMA, as illustrated by the Mulliken charges for the different fragments reported in Fig. 2. This effect is larger for the complexes with indole, where the TMA charge is + 0.97|e$^-$|, than for the other two.

Looking at the energy differences given in Table 2 for the TMA complexes in the presence of the PCM field, the most striking feature is a lowering of all the interactions energies. This result can be rationalized in terms of two concurrent effects. On one hand, the bulk solvent reduces the charge-transfer component to the interaction energy (thus increasing the role of the dispersion forces), while on the other, it mimics the interactions of TMA with water solvent molecules. This latter is stronger than the contact with the aromatic ring. As a consequence, the initial values, corresponding to gas-phase calculations, are drastically reduced in a continuum model of the solvent (compare the first and fourth rows of Table 2). However, the sequence of interaction energies computed for water present is the same as without a solvent. Effects due to possible ZVPE variations are not significant.

As in the gas-phase systems, a full optimization of all the parameters for the TMA–benzene complex does not induce any significant variation either in the geometrical parameters or in the interaction energy. For instance, the distance is the same as in the gas-phase, while the interaction energy decreases by 0.2 kcal mol^{-1} with respect to the value computed for the gas phase. These results well underline the use of "frozen" structures for all the other calculations.

As mentioned earlier, the continuum model, as the one considered in the present paper, only partially mimics the effects of strong and specific solute–solvent interactions. These effects are particularly important in a polar solvent (like water), where at least the first solvation shell has to be considered in order to correctly reproduce solute physicochemical properties [26]. So, to better elucidate the problem of the hydration of TMA complexes, we investigated the effects resulting from additional H$_2$O molecules fixed on some of the previously mentioned systems and, eventually, to be plunged in the dielectric continuum simulating the bulk water. In this last case, of course, the cavities involved in the final PCM treatment have to be reconstructed and the total energies have to be reevaluated accordingly. To do that, TMA, either isolated or complexed, was surrounded by three H$_2$O molecules located in the first three bisector planes of the cations, in such a way that the approach of the N$^+$ atom can be effected by the fourth side (Fig. 3). For the substrates only the possible formation of a hydrogen bond between the NH group of indole and one H$_2$O molecule was taken into account. This molecule strongly interacts with the nitrogen atom of the NH group, the corresponding binding energy being 5.9 kcal mol^{-1}, about half of the TMA–H$_2$O interaction (10.9 kcal mol^{-1} for TMA–H$_2$O after BSSE correction). At the same time, this contact is still competitive with respect the water–water interaction (about 5.0 kcal mol^{-1} [39]). However, the presence of further solvent molecules bonded less strongly (especially those interacting with the aromatic cycles) might be considered, but in such an eventuality solvent–solvent interaction may become competitive [40]. These phenomena could be treated only in the framework of a quantum dynamics study, which is well beyond the scope of the present work.

The three explicit water molecules affect the intermolecular rearrangement in a more significant way than the bare continuum model, the intermolecular distance being slightly more stretched. This effect is more evident for the TMA–phenol adduct (+0.07 Å) than for the

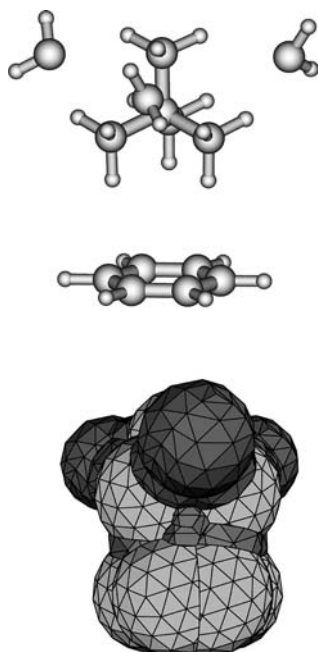**Fig. 4.** Structure of the TMA–indole–benzene complex

Fig. 3. Structure of the adduct TMA plus three water molecules plus benzene (*left*) and sketch of the corresponding cavity (*right*) used in the polarizable continuum medium approach

Table 3. Different contribution to the interaction energies between TMA $+ 3H_2O$ and the aromatic molecules considered (kcal/mol). ΔE_{solv} was computed using the DPCM approach (see text for details)

	Benzene	Phenol	Indole	Indole $+ H_2O$
ΔE_{gas}	8.2	9.7	12.1	15.2
BSSE	−2.6	−3.5	−3.9	−4.2
ΔE_{solv}	−3.9	−4.4	−5.1	−8.1
Total	1.7	1.8	3.1	2.9

other systems. It is interesting to note that, anyway, both continuum and supermolecular approaches show the same trend (lengthening of the N–ring distances). At the same, the small difference observed between the two models, $+0.02$ Å in the indole complex, $+0.01$ Å for phenol and $+0.04$ Å for benzene, can be related to the electron-withdrawing effect through the hydrogen bonds, a mechanism ruling the solute–water interaction in the cluster. The positive charge on the water molecule ($+0.03 |e^-|$), well underlines such behavior. The overall effect is a significant decrease of the positive charge located on the TMA: from $+0.94 |e^-|$ in the TMA–benzene complex to $0.86 |e^-|$ in the corresponding adduct with three water molecules.

When the TMA–aromatic–water adduct is plunged in the continuum model, in order to simulate the solvation shell beyond the first, no significant variations of the molecular properties are observed. In fact, a glance at the results listed in Table 3 shows that the lowering of the binding energy of TMA with aromatics as a consequence of hydration is a little less important than
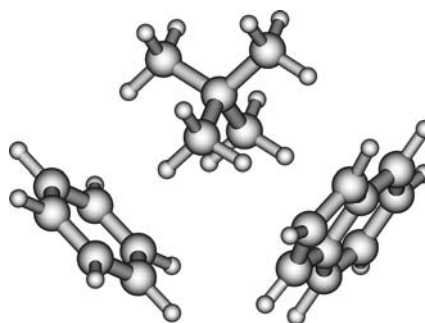
previously. Two different factors are operative in this more sophisticated model: first, a part of the solvation effect is transferred to the primitive supermolecule calculations; second, the lowering of the PCM contributions to solvation energies is in line with the increasing size of the cavities, but the interplay of both contributions does not affect, qualitatively speaking, the final balance very much. It can be added that a similar lowering of the binding energy of TMA with benzene has also been found in Monte Carlo simulations using the semiempirical AM1 potential [18], but to a larger extent than our PCM ab initio approach.

As concerns the other parameters considered, that is intermolecular distances and TMA charge, the continuum model does not introduce any perturbation, thus underlining the negligible contribution of the solvation shells beyond the first one to such parameters.

In summary, our conclusion shows that the PCM model provides, at least, reliable trends for the energetics and the geometrical features of the TMA–aromatic adducts and the explicit consideration of water solvent molecules does not affect the results, even when a cation such TMA is present.

In order to finally assess the problem of cation–π interactions and to better reproduce probable biological situations, we also investigated, in a last series of calculations, the possibility of having cation–π complexes with two aromatic molecules, each of them being linked by three hydrogens belonging to TMA. This kind of structure is preserved in the benzene–TMA–indole system depicted in Fig. 4; this is due to the fact that starting, for instance, from the TMA–indole complex, there are still three CH bonds which are able to interact laterally with benzene (and vice-versa). Following our previous results on the different TMA-aromatic pairs, this structure was built up starting from the single fragments and optimizing only the two N–ring distances as well as the angle defined by them.

These distances do not significantly differ from those obtained in the two corresponding dimers, being 4.15 and 4.22 Å for TMA–indole and TMA–benzene, respectively. Concerning the magnitude of the interaction between TMA and the benzene–indole pair, we found that the affinity of this ion for benzene is not lowered very much if it is previously attached to indole

(or the reverse). The dissociation energy of the complex with respect to its three components is close to the sum of the binding energy of TMA with benzene and indole (26.5 kcal mol^{-1} in the gas phase before BSSE corrections instead of 27.3 kcal mol^{-1}). In a similar manner, solvation has the same effect as for the two separate dimers, so the total interaction energies are only slightly lower (cf. last two columns of Table 2). These last points may be interesting in connection with data coming from laboratory analogues of biological receptors.

Conclusions

To conclude, it appears that the relative affinities of the aromatic rings of phenylalanine, tyrosine and tryptophan for modeling the binding of the quaternary ammonium group in TMA remains in the same order after introduction of the solvent in spite of an important reduction (by about three quarters) of their magnitude in the gas phase. Although the amount of this reduction depends clearly on the characteristics of the theoretical model used to describe hydration, such an effect seems reasonable in making the binding energies more compatible with the necessary lability of transient biological interactions.

References

1. Deakyne CA, Meot-Ner M (1985) J Am Chem Soc 107:474
2. Dougherty DA, Stauffer DA (1990) Science 250:1558
3. Satow YGH, Cohen EA, Padlan DR, Davies J (1986) J Mol Biol 190:593
4. Galzi JL, Revah F, Bessis A, Changeux JP (1991) Annu Rev Pharmacol 31:377
5. Sussman JL, Harel M, Frolow F, Defner C, Goldman A, Toker L, Silma L (1991) Science 253:872
6. Pullman A, Xiao-Wen H (1994) Biophys J 66:345
7. Furois-Corbin S, Pullman A (1989) Biochim Biophys Acta 984:339
8. Pullman A (1995) In Pullman A et al (eds) Modelling of biomolecular structures and mechanics. Kluwer, Dordrecht, pp
9. Ma JC, Dougherty DA (1997) Chem Rev 97:1303, and references therein
10. Pullman A, Berthier G, Savinelli R (1997) J Comput Chem 18:2012
11. Berthier G, Savinelli R, Pullman A (2000) Theor Chem Acc 104:78
12. Pullman A, Berthier G, Savinelli R (1998) J Am Chem Soc 120:8553
13. Pullman A, Berthier G, Savinelli R (2001) J Mol Struct (THEOCHEM) 537:103
14. Mecozzi S, West AP, Dougherty DA (1996) Proc Natl Acad Sci USA 93:10566
15. Pullman B, Berthod H, Gretsh N (1975) Acad Sci Paris D 280:1741
16. Rao BG, Singh UC (1989) J Am Chem Soc 111:3125
17. Gao J, Chou LW, Auerbach A (1993) Biophys J 65:43
18. Duffy EM, Kowalzyk PJ, Jörgensen WJ (1993) J Am Chem Soc 115:9271
19. Garcia-Torrés L, Guàrdia E (1998) J Phys Chem B 102:7448
20. Miertus S, Scrocco E, Tomasi J (1981) Chem Phys 55:117
21. Cossi M, Barone V, Cammi R, Tomasi J (1996) Chem Phys Lett 255:327
22. Tomasi J, Persico M (1994) Chem Rev 94:2027
23. Cramer CJ, Truhlar DG (1999) Chem Rev 99:2161
24. Adamo C, Cossi M, Rega N, Barone V (2001) In: Eriksson LA (ed) Theoretical Biochemistry – Processes and Properties of Biological Systems, Elsevier, The Netherlands, pp 467
25. Bartoli S, Roelens S (1999) J Am Chem Soc 121:11908
26. Adamo C, di Matteo A, Rey P, Barone V (1999) J Phys Chem A 103:3481
27. Chalmet S, Ruiz-Lopez MF (2001) J Chem Phys 115:5220
28. Ciofini I, Adamo C (2001) J Phys Chem A 105:1086
29. Mennicci B, Toniolo A, Tomasi J (2001) J Phys Chem A 105:7126
30. Boys SF, Bernardi F (1970) Mol Phys 19:553
31. Møller C, Plesset MS (1934) Phys Rev 46:618
32. Grev RS, Janssen CL, Schaeffer HF III (1991) J Chem Phys 95:5128
33. Curtiss LA, Pople JA (1975) J Mol Phys 55:1
34. Barone V, Cossi M, Tomasi J (1998) J Comput Chem 19:407
35. Rivail JL, Rinaldi D (1976) Chem Phys 18:233
36. Cossi M, Rega, N, Scalmani G, Barone V (2001) J Chem Phys 114:5691, and references therein
37. Frisch MJ, Trucks GW, Schlegel HB, Scuseria GE, Stratmann RE, Burant JC, Dapprich S, Millam JM, Daniels AD, Kudin KN, Strain MC, Farkas O, Tomasi J, Barone V, Cossi M, Cammi R, Mennucci B, Pomelli C, Adamo C, Clifford S, Ochterschi J, Cui Q, Gill PMW, Johnson BG, Robb MA, Cheeseman JR, Keith T, Petersson P, Morokuma K, Malick DK, Rabuck AD, Montgomery JA, Raghavachari K, Al-Laham MA, Zakrewski VG, Ortiz JV, Foresman JB, Cioslowski J, Stefanov BB, Nanayakkara A, Liu J, Liashenklo A, Piskorz P, Komaromi I, Challacombe M, Peng CY, Ayala PY, Chen W, Wong MW, Andres JL, Replogle ES, Gomperts R, Martin RL, Fox DJ, Binkley JS, DeFrees DJ, Baker J, Stewart JP, Head-Gordon M, Gonzalez C, Pople JA (1998) Gaussian 98, revision A.7. Gaussian, Pittsburgh, PA
38. Felder C, Jiang HL, Zhu WL, Chen KX, Silman I, Botti SA, Sussman JL (2001) J Phys Chem A 105:1326
39. Barone V, Orlandini L, Adamo C (1994) Chem Phys Lett 231:295
40. Pasquarello A, Petri I, Salmon PS, Parisel O, Car R, Toth E, Powell EH, Fischer HE, Helm L, Merbach AE (2001) Science 291:856